

5-2017

PARP inhibitor upregulates PD-L1 expression and enhances cancer-associated immunosuppression

Shiping Jiao

Follow this and additional works at: https://digitalcommons.library.tmc.edu/utgsbs_dissertations



Part of the [Cancer Biology Commons](#), [Medical Immunology Commons](#), [Neoplasms Commons](#), and the [Oncology Commons](#)

Recommended Citation

Jiao, Shiping, "PARP inhibitor upregulates PD-L1 expression and enhances cancer-associated immunosuppression" (2017). *The University of Texas MD Anderson Cancer Center UTHealth Graduate School of Biomedical Sciences Dissertations and Theses (Open Access)*. 739.
https://digitalcommons.library.tmc.edu/utgsbs_dissertations/739

This Thesis (MS) is brought to you for free and open access by the The University of Texas MD Anderson Cancer Center UTHealth Graduate School of Biomedical Sciences at DigitalCommons@TMC. It has been accepted for inclusion in The University of Texas MD Anderson Cancer Center UTHealth Graduate School of Biomedical Sciences Dissertations and Theses (Open Access) by an authorized administrator of DigitalCommons@TMC. For more information, please contact digitalcommons@library.tmc.edu.

**PARP INHIBITOR UPREGULATES PD-L1 EXPRESSION AND ENHANCES
CANCER-ASSOCIATED IMMUNOSUPPRESSION**

By

Shiping Jiao M.D.

APPROVED

Advisory Professor: Mien-Chie Hung Ph.D.

Liuqing Yang Ph.D.

Jeffrey T. Chang Ph.D.

Zhen Fan M.D.

Guang Peng M.D. Ph.D.

APPROVED

Dean, The University of Texas

MD Anderson Cancer Center UTHHealth Graduate School of Biomedical Sciences

**PARP inhibitor upregulates PD-L1 expression and enhances
cancer-associated immunosuppression**

A

THESIS

Presented to the Faculty of
The University of Texas
MD Anderson Cancer Center UTHealth
Graduate School of Biomedical Sciences
in Partial Fulfillment

of the Requirements

for the Degree of

MASTER OF SCIENCE

By

Shiping Jiao M.D.

Houston, Texas

May 2017

Dedication

To

My dearest parents, Xin Jiao and Jie Chen

My wife Cheng Peng

And my son Longyuan Jiao

Acknowledgements

Firstly I appreciate Dr. Mien-Chie Hung, for accepting me to do research in his lab, and for supervising me in this project. Thank Dr. Mien-Chie Hung, Dr. Liuqing Yang, Dr. Jeffrey T. Chang, Dr. Zhen Fan and Dr. Guang Peng to serve as my advisory committee, and to provide valuable suggestions to my project. I especially thank Dr. Hung, Dr. Chang and Dr. Yang gave me strong recommendation letters when I applied the Ph.D. program. I also thank the colleagues in Dr. Hung's lab, and we have good time although the wet bench work is exhausting. Thank GSBS staff, especially Ms. Brenda Gaughan, who is always helpful when I have questions about academic affairs. I greatly thank my wife Cheng Peng and my parents, for supporting me always, and for taking care of the family.

PARP INHIBITOR UPREGULATES PD-L1 EXPRESSION AND ENHANCES CANCER-ASSOCIATED IMMUNOSUPPRESSION

Abstract

Shiping Jiao, M.D.

Advisory Professor: Mien-Chie Hung, Ph.D.

With recent approvals for therapeutic antibodies that block CTLA4, PD-1 and PD-L1, immune checkpoints have emerged as new targets in cancer therapy. In addition, there is accumulating evidence highlighting the role of cancer-associated immunity in patient response to cytotoxic anticancer agents. Inhibitors of poly (ADP-ribose) polymerase (PARP) have shown substantial cytotoxic effects against tumors with defects in DNA damage responses. However, whether a crosstalk between PARP inhibition and immune checkpoints exists remains unclear. Here, it has been shown that PARP inhibitors (PARPi) upregulate PD-L1 expression in multiple cancer cell lines, human xenograft tumors and syngeneic mouse tumors. Mechanistically, PARPi inactivates GSK3 β , which in turn enhances PARPi-mediated PD-L1 upregulation. PARPi attenuates anticancer immunity via upregulation of PD-L1, and blockade of PD-L1 re-sensitizes

PARPi-treated cancer cells to T cell killing. The combination of PARPi and anti-PD-L1 therapy compared with each agent alone significantly increased the therapeutic efficacy in vivo. In details, PARPi treatment increases T lymphocytes infiltration in tumors; however the induced PD-L1 by PARPi on cancer cells inhibits the activation of the infiltrating T lymphocytes. Thus, the addition of PD-L1 blockade to PARPi therapy can re-activate anti-tumor immunity and improve the therapeutic efficacy. This study demonstrates a crosstalk between PARPi and tumor-associated immunosuppression, and provides a rationale for the combination of PARPi and PD-L1 or PD-1 immune checkpoint blockade as a potential therapeutic approach. (Jiao et al., 2017)

Table of Contents

APPROVAL SHEET	III
TITLE	III
DEDICATION	III
ACKNOWLEDGEMENTS	IV
ABSTRACT	V
TABLE OF CONTENT	VII
LIST OF ILLUSTRATIONS	XI
CHAPTER 1 INTRODUCTION	1
1.1 PARP and PARP inhibitor	2
1.2 Combination strategies to potentiate PARP inhibitor	2
1.3 Cancer-associated immunity and immune checkpoint therapy.....	4
1.4 Cytotoxic anticancer agents and cancer-associated immunity	5

CHAPTER 2	MATERIALS AND METHODS.....	6
2.1	Cell lines	7
2.2	Antibodies and Chemicals.....	7
2.3	Human phospho-kinase antibody array	8
2.4	Detection of cell surface PD-L1.....	8
2.5	PD-L1/PD-1 binding assay	9
2.6	T-cell killing assay	9
2.7	PD-L1 detection in xenograft tumors.....	10
2.8	Syngeneic tumor model treatment protocol.....	11
2.9	Tumor cell PD-L1 expression and tumor-infiltrating lymphocyte analysis.....	11
2.10	Immunohistochemical staining (IHC) of human breast tumor tissue samples..	12
2.11	Statistical Analysis	13
CHAPTER 3	RESULTS AND ANALYSIS.....	14
3.1	PARPi upregulates PD-L1 <i>in vitro</i> and <i>in vivo</i>	15

3.1.1	PARPi upregulates PD-L1 <i>in vitro</i>	15
3.1.2	PARPi upregulates PD-L1 in both BRCA proficient and deficient cancer cells	16
3.1.3	PARPi upregulates PD-L1 <i>in vivo</i>	19
3.3	PARPi-induced PD-L1 upregulation is primarily via GSK3β inactivation	23
3.3	PARPi attenuates T-cell killing through PD-L1 induction	23
3.3.1	PARPi attenuates T-cell killing	23
3.3.2	Anti-PD-L1 re-sensitizes cancer cells treated with PARPi to T-cell killing	27
3.4	Combination with PD-L1 blockade sensitizes PARPi therapy	28
3.5	Correlations of PARylation and PD-L1 expression in human tumor tissues.....	33
3.6	PARPi treatment increases T lymphocytes infiltration in tumors.....	35
3.7	PARPi upregulates PD-L1 in specific cancer cell lines	37

CHAPTER 4	CONCLUSION AND DISCUSSION	40
CHAPTER 5	BIBLIOGRAPHY	44
CHAPTER 6	VITA.....	55

List of Illustrations

Figure 1. PARPi upregulates PD-L1 protein expression in breast cancer cells.	17
Figure 2. Effects of downregulation of BRCA1/2 on PARPi-induced PD-L1.	18
Figure 3. PARPi upregulates PD-L1 expression in xenograft tumors.	20
Figure 4. PARPi upregulates PD-L1 primarily via GSK3 β inactivation.	23
Figure 5. Olaparib attenuates T-cell-mediated cell death in TNBC cells.	25
Figure 6. PARPi inhibits MDA-MB-231 proliferation but not PBMCs.	27
Figure 7. PARPi combined with PD-L1 blockade in syngeneic mouse model.....	30
Figure 8. Toxicity assessment of treatment on BALB/c mice.	32
Figure 9. PAR inversely correlates PD-L1 in breast cancer specimens.....	34
Figure 10. PARPi increases T lymphocytes infiltration in EMT6 tumors.	36
Figure 11. PARPi upregulates PD-L1 in specific cancer cell lines.....	38
Figure 12. A more obvious induction of PD-L1 in EMT6 cells than 4T1 cells.....	39

Chapter 1 Introduction

1.1 PARP and PARP inhibitor

Poly (ADP-ribose) polymerase (PARP) engages in DNA base excision repair by inducing poly (ADP-ribose)lation of itself and other target proteins (Sonnenblick et al., 2015). In addition, PARP has a less well-defined role in homologous recombination mediated (Bryant et al., 2009) and alternative non-homologous end-joining mediated double-strand break repair (Paddock et al., 2011). PARP inhibition has been shown to be an effective therapeutic strategy against tumors associated with germline mutations in double-strand DNA repair genes by inducing synthetic lethality (Sonnenblick et al., 2015). One PARP inhibitor (PARPi), olaparib, was approved by the U.S. Food and Drug Administration (FDA) in 2014 for the treatment of germline *BRCA*-mutated (gBRCAm) advanced ovarian cancer (Kim et al., 2015). More recently, another PARPi, niraparib, which was shown to significantly prolong the progression-free survival in ovarian cancer patients, received a fast track designation from the FDA for the treatment of patients with recurrent platinum-sensitive ovarian cancer (Mirza et al., 2016).

1.2 Combination strategies to potentiate PARP inhibitor

In addition to ovarian cancer, PARPi has demonstrated tremendous potential in breast cancer, and there are currently several active clinical trials evaluating PARPi-containing

combination therapies for advanced breast cancer. Although the objective response rate to PARPi in patients with advanced breast cancer harboring BRCA1/2 mutations was reported as high as 41%, its response duration is still very limited with a 5.7-month median duration (Tutt et al., 2010). The underlying resistance mechanisms to PARPi have mainly attributed to the restoration of double-strand break repair. For instance, secondary BRCA mutations that restore BRCA function (Edwards et al., 2008) and reduced 53BP1 expression leading to partial restoration of homologous recombination (Jaspers et al., 2013) have been described as the potential resistance mechanisms to PARPi. In order to enhance the cytotoxic effect of PARPi, several combinations of PARPi and targeted anticancer agents, such as inhibitors against phosphatidylinositol 3-kinase (Ibrahim et al., 2012; Juvekar et al., 2012), Wee1 kinase (Karnak et al., 2014), DNA topoisomerase I (Kummar et al., 2011), and DNA methyltransferase (Muvarak et al., 2016), have been proposed. In addition, c-Met-mediated phosphorylation of PARP was reported to contribute to PARPi resistance, suggesting that the combined inhibition of c-Met and PARP may benefit patients who do not respond to PARPi and whose tumors are associated with c-Met activation (Du et al., 2016). Thus, developing a rational combination therapy with PARPi may lead to effective anticancer strategy.

1.3 Cancer-associated immunity and immune checkpoint therapy

Over the last few years, there have been major breakthroughs in our understanding of tumor-associated immunosuppression. A key mechanism underlying cancer immune evasion is the expression of multiple inhibitory ligands, notably PD-L1, on the surface of cancer cells. Engagement of the PD-1 receptor on T cells by PD-L1 leads to the suppression of T cell proliferation, cytokine release, and cytolytic activity whereas blockade of co-inhibitory ligation with monoclonal antibodies, such as PD-L1 or PD-1 antibodies, restores T cell function and increases therapeutic efficacy (Dong et al., 2002; Freeman et al., 2000). The impressive and durable clinical response of checkpoint blockade immunotherapy resulted in the FDA approval of ipilimumab, nivolumab, pembrolizumab, and more recently atezolizumab for the treatment of multiple types of cancer, such as melanoma, Hodgkin's lymphoma, and lung and bladder cancers ((Garon et al., 2015; Hodi, 2010; Robert et al., 2015; Rosenberg et al., 2016)). Notably, the PD-1 antibody pembrolizumab was approved as first-line treatment for patients with advanced non-small cell lung cancer and high PD-L1 expression (Reck et al., 2016).

1.4 Cytotoxic anticancer agents and cancer-associated immunity

There is accumulating evidence indicating that conventional and targeted anticancer therapies also affect tumor-targeting immune responses (Galluzzi et al., 2015). Thus, delineating the crosstalk between cytotoxic anticancer agents and cancer-associated immunity may lead to more efficient combinatorial regimens. Although the effects of PARPi, a targeted anticancer agent, have shown promising results in multiple cancer types, how and whether PARPi plays a role in cancer-associated immunity is still unknown. In the current study, I investigate the crosstalk between PARP inhibition and immune checkpoint, in particular, the PD-L1/PD-1 axis, which is a dominant immune checkpoint pathway in the tumor microenvironment, and further explore a mechanism-driven combination strategy to potentiate PARPi.

Chapter 2 Materials and Methods

2.1 Cell lines

All cell lines were obtained from ATCC (Manassas, VA) and have been independently validated by STR DNA fingerprinting at MD Anderson Cancer Center. PARP1 (#sc-400046), PD-L1 (#sc-401140), and GSK3 β (#sc-425249) knockout cells were established using CRISPR/Cas9 KO plasmids from Santa Cruz Biotechnology (Dallas, TX). PARP1 knockdown MDA-MB-231 cells were established as described previously (Du et al., 2016).

2.2 Antibodies and Chemicals

PD-L1 (#13684), PARP1 (#9532), phospho-GSK3 β (Ser9, #9336), GSK3 β (#9315), Ki-67 (#9449) antibodies were purchased from Cell Signaling Technology, BRCA1 (sc-8326) and BRCA2 (sc-642) were from Santa Cruz, and α -Tubulin (#B-5-1-2) and β -Actin (#A2228) were obtained from Sigma-Aldrich (St. Louis, MO). CD3 (ab5690) were purchased from Abcam. Olaparib, rucaparib, and talazoparib were purchased from Selleckchem (Houston, TX), ChemieTek (Indianapolis, IN), and Selleckchem, respectively. The Human Phospho-Kinase Array Kit (#ARY003B) was purchased from R&D Systems (Minneapolis, MN) and human CD274 (B7-H1, PD-L1) antibody for T-cell killing assay was from BioLegend (#329709). eSiRNA human BRCA1 (EHU096311), eSiRNA human BRCA2 (EHU031451) and siRNA universal negative control (SIC001) were from Sigma-Aldrich.

2.3 Human phospho-kinase antibody array

The Human Phospho-Kinase Array Kit (#ARY003B) was from R&D Systems (Minneapolis, MN). Array screening was performed following the manufacturer's manuals. In brief, cell lysates were incubated with the array membranes. After washing, membranes were incubated with biotinylated antibody cocktail. The amounts of phospho-kinase were assessed with streptavidin conjugated to horseradish peroxidase, followed by chemiluminescence detection. The software GS-800 Calibrated Densitometer (Bio-Rad Laboratories, CA) was utilized to quantify the density of each dot against the average of the internal controls on the membrane as indicated in the protocol.

2.4 Detection of cell surface PD-L1

For detection of cell surface PD-L1, cells were suspended in 100 μ l of cell staining buffer (#420201, BioLegend) and incubated with APC conjugated anti-human PD-L1 antibody (#329708, BioLegend) at room temperature for 30 min. After washing in the staining buffer, stained cells were analyzed by fluorescence-activated cell sorting (FACS; BD Biosciences).

2.5 PD-L1/PD-1 binding assay

Cells (1×10^6) were incubated with 5 $\mu\text{g/ml}$ recombinant human PD-1 FC chimera protein (#1086-PD-050, R&D Systems) at room temperature for 30 min. After washing in staining buffer, cells were incubated with anti-human Alexa Fluor 488 dye conjugated antibody (ThermoFisher Scientific) at room temperature for 30 min. Cells were analyzed by FACS after wash in the staining buffer. The FACS data was analyzed using Flowjo (Tree star, CA), and the cutoff line for relative positive percentage was set at the median of the maximum signal.

2.6 T-cell killing assay

NucLight RFP MDA-MB-231 cells (#4457, Essen Bioscience, Ann Arbor, MI) were seeded in a 96-well plate with or without olaparib. Human peripheral blood mononuclear cells (PBMCs; #70025, STEMCELL, Vancouver, BC, Canada) were activated with 100 ng/ml CD3 antibody, 100 ng/ml CD28 antibody and 10 ng/ml IL-2 (#317303; #302913; #589102, BioLegend, San Diego, CA) and then co-cultured with MDA-MB-231 cells at 10:1 ratio in the presence of fluorescence caspase 3/7 substrate (#4440, Essen Bioscience).

2.7 PD-L1 detection in xenograft tumors

All animal procedures were conducted under the guidelines approved by the Institutional Animal Care and Use Committee (IACUC) at UT MD Anderson Cancer Center. MDA-MB-231 (0.5×10^6), BT549 (1×10^6) or SUM149 (2×10^6) cells in Matrixgel (BD Biosciences, San Jose, CA) were inoculated in the mammary fat pads of nude mice (6 – 8 weeks, female). When tumor volume reached $\sim 50 \text{ mm}^3$, mice were administered olaparib (25 mg/kg) or rucaparib (5 mg/kg) orally 5 days per week for three weeks. Tumors were harvested after final treatment, and analyzed by immunoblotting and immunohistochemistry (IHC). IHC staining was as described previously (Xia et al., 2004). Briefly, frozen tissue sections were fixed with 4% paraformaldehyde for 1 hour and then hydrated in PBS for 5 min at room temperature (RT). Sections were permeabilized with 0.5% triton X-100 for 15 min at RT. The endogenous peroxidase activity was blocked with 0.3% hydrogen peroxide in methanol for 15 min at RT. After serum blocking, the slides were incubated overnight at 4 °C with human PD-L1 antibody (#13684, Cell Signaling Technology, 1:50 dilution). Slides were then incubated with biotinylated secondary antibodies for 1 hour at RT, followed by incubation with avidin-biotin-horseradish peroxidase complex. Visualization was performed

using 0.125% amino-ethylcarbazole chromogen. After counterstaining with Mayer's hematoxylin, slides were mounted.

2.8 Syngeneic tumor model treatment protocol

BALB/c mice (6–8 week female, Jackson Laboratories, Bar Harbor, Maine) were inoculated in the mammary fat pads with EMT6 (1×10^5) cells in Matrixgel. On days 3 after the inoculation, mice were injected intraperitoneally with 50 mg/kg olaparib or vehicle daily. After days 4, mice were injected intraperitoneally every 4 days with 75 μ g anti-mouse PD-L1 antibody (10F.9G2, Bio X cell) or control rat IgG2b (LTF-2, Bio X cell). Tumor volumes were measured every 3 days with a digital caliper, and were calculated using the formula: $\pi/6 \times \text{length} \times \text{width}^2$. Body weight was measured every 5 days.

2.9 Tumor cell PD-L1 expression and tumor-infiltrating lymphocyte (TIL) analysis

EMT6 tumors were excised and digested in collagenase/hyaluronidase and DNase I, and dissociated by gentleMACS Dissociator as described by the protocol of tumor dissociation kit (Miltenyi Biotec, Auburn, CA). Tumor cells and TIL were enriched and harvested separately by Percoll gradient (Sigma). Cell Surface PD-L1 of Tumor cell were stained with Brilliant Violet 421-conjugated anti-mouse PD-L1 antibody (#124315,

BioLegend) and analyzed by FACS, and TIL were stained and analyzed by mass cytometry (CyTOF). The antibodies used to stain TIL were listed as followed: CD45-147Sm; CD3e-152Sm; CD4-172Yb; CD8a-168Er; IFN γ -165Ho (Fluidigm, CA).

2.10 Immunohistochemical staining (IHC) of human breast tumor tissue samples

IHC staining was performed as described previously (Lim et al., 2016). Human breast tumor tissue specimens were obtained following the guidelines approved by the Institutional Review Board at MD Anderson, and written informed consent was obtained from patients in all cases. Briefly, tissue specimens were incubated with antibodies against PAR (Enzo Life Science, Clone 10H, 1:200 dilution) and PD-L1 (Abcam, Clone 288, #ab205921, 1:100 dilution) and a biotin-conjugated secondary antibody and then incubated with an avidin–biotin–peroxidase complex. Visualization was performed using amino-ethylcarbazole chromogen. According to the histological scores, the intensity of staining was ranked into four groups: high (+++), medium (++), low (+) and negative (–).

2.11 Statistical Analysis

Statistical analyses were performed using GraphPad Prism software (GraphPad, San Diego, CA). Student's *t*-test or one-way analysis of variance (ANOVA) were used to compare experimental data. The Pearson Chi-square test were used to analyze IHC data. A P value < 0.05 (*) was considered statistically significant.

Chapter 3

Results and Analysis

3.1 *PARPi upregulates PD-L1 in vitro and in vivo*

3.1.1 *PARPi upregulates PD-L1 in vitro*

Elevated PD-L1 expression in cancer cells has been shown to enhance PD-L1/PD-1 axis-mediated anticancer immunosuppression (Dong et al., 2002; Reck et al., 2016). To determine whether inhibition of PARP affects the PD-L1 protein level, we treated MDA-MB-231 and BT549 cells with two different PARP inhibitors (PARPi), olaparib and talazoparib, and determined PD-L1 expression by immunoblotting. PARPi treatment increased the total level of PD-L1 protein in both cell lines (Fig. 1A). To validate whether PARPi-induced PD-L1 upregulation is through PARP1 inhibition, we knocked down (K/D) or knocked out (K/O) PARP1 in MDA-MB-231 cells. Consistent with the results shown in Figure 1A, PD-L1 expression in the PARP1 knockdown and knockout cells was substantially higher compared with the parental cells (Fig. 1B).

PD-L1 expressed on cell surface of cancer cells exerts immunosuppressive effects by binding to PD-1 receptor on activated T cells (Topalian et al., 2012). To determine whether the level of cell surface PD-L1 increases after PARPi treatment, MDA-MB-231 cells were treated with or without PARPi and subjected to FACS using fluorescence-labeled PD-L1 antibody. Cell surface PD-L1 levels have significantly increased after olaparib and talazoparib treatment (Fig. 1C, left panel). Likewise, cell surface PD-L1 levels were higher

in PARPi knockdown and knockout MDA-MB-231 cells than in parental cells (Fig. 1C, right panel).

3.1.2 PARPi upregulates PD-L1 in both BRCA proficient and deficient cancer cells

Because PARPi is commonly used to treat *BRCA*-deficient cancers (Kaufman et al., 2015), we also investigated the effects of olaparib on *BRCA*-mutant SUM149 cells. SUM149 cells were treated with the different concentrations of olaparib for 10 days to mimic chronic PARPi exposure in clinic, and subjected to FACS to determine PD-L1 expression. Consistent with the results in MDA-MB-231 cells, cell surface PD-L1 was significantly increased following olaparib treatment in a dose-dependent manner (Fig. 1D). To further validate the role of *BRCA* deficiency in PARPi-induced PD-L1 upregulation, we knocked down *BRCA1* or *BRCA2* in MDA-MB-231 cells and exposed cells to olaparib. Downregulation of *BRCA1* or *BRCA2* had virtually no effect on PARPi-induced PD-L1 expression (Fig. 2). These results together suggested that PARPi can upregulate cell surface PD-L1 level in both *BRCA*-proficient and *BRCA*-deficient cells.

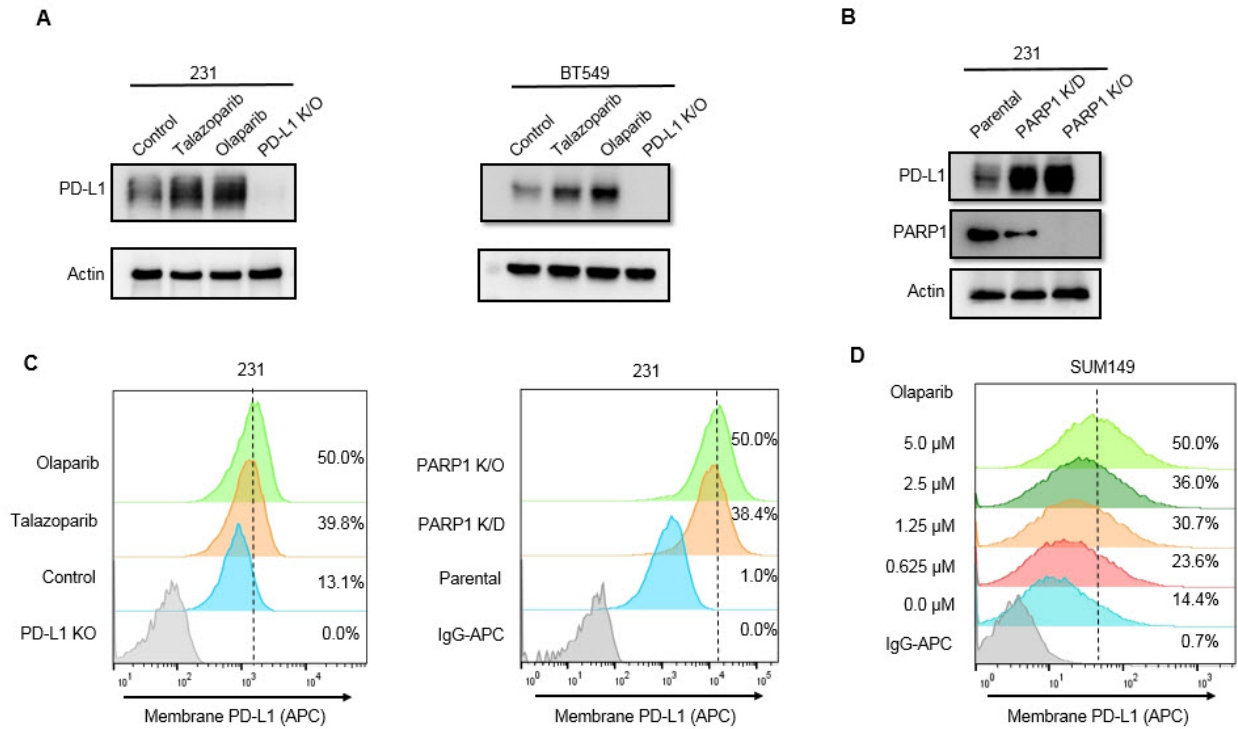


Figure 1. PARPi upregulates PD-L1 protein expression in breast cancer cells. (A)

MDA-MDA-MB-231 and BT549 cells were treated with 10 μ M olaparib or 10 nM talazoparib for 24 hours, and subjected to immunoblotting with the indicated antibodies. PD-L1 knockout (K/O) cells were included as a negative control. (B) PD-L1 expression in

PARP1 knockdown (K/D), PARP1 knockout (K/O), and MDA-MB-231 parental cells by immunoblotting. (C and D) The indicated MDA-MB-231 cells were subjected to FACS analysis for cell surface PD-L1 expression. (E) SUM149 cells were treated with the

indicated concentrations of olaparib for 10 days, and cell surface PD-L1 expression was determined by FACS.

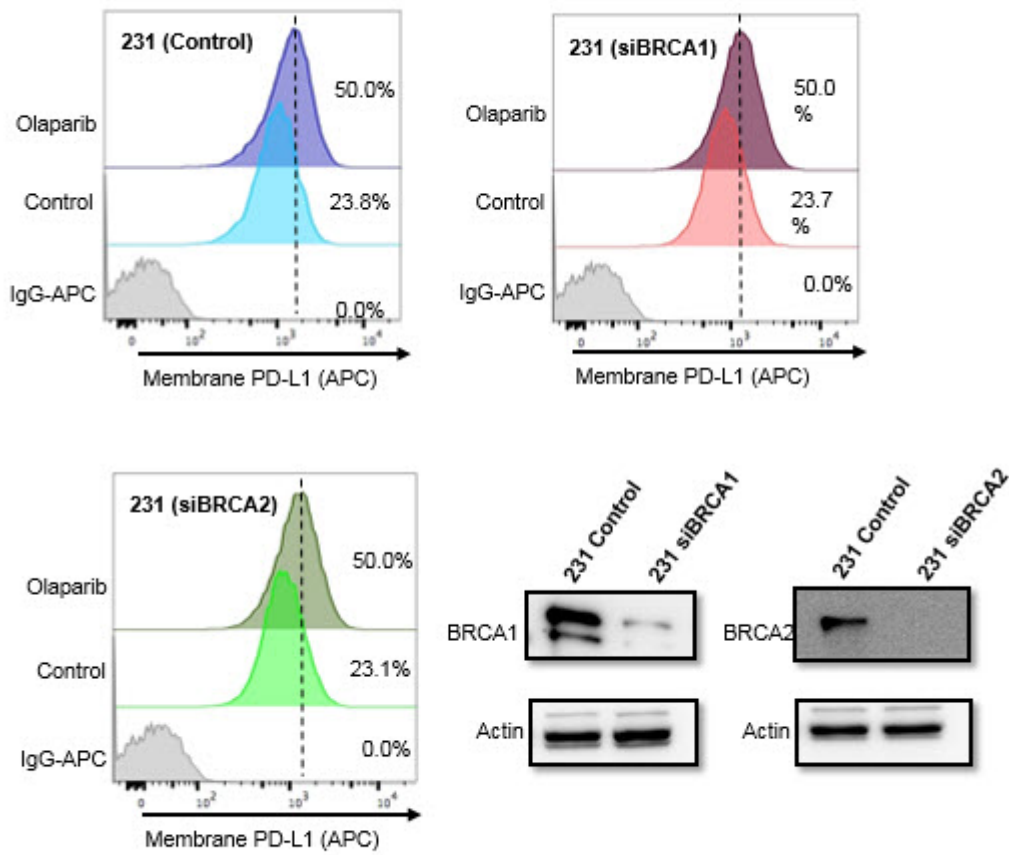


Figure 2. Downregulation of BRCA1 or BRCA2 has no effect on PARPi-induced PD-L1 upregulation. MDA-MB-231 cells were transfected with the indicated siRNA to knock down *BRCA1* or *BRCA2*. After 36 hours of transfection, cell were treated with 10 μ M olaparib for 24 hours and subjected to FACS analysis. MDA-MB-231 cells stained with IgG-APC were set as isotype controls. Western blot showing *BRCA* knockdown by siRNA.

3.1.3 PARPi upregulates PD-L1 in vivo

Next we asked whether PARPi may affects PD-L1 expression in tumors, we inoculated BT549 and SUM149 cells into the mammary fad pads of nude mice, and after tumor formed, administered olaparib to mice 5 days a week for 3 weeks. Tumor tissues from xenografts were isolated and subjected to immunoblotting with PD-L1 antibody. As shown, PD-L1 expression was substantially higher in the xenograft tumors from mice treated with olaparib compared with those from the untreated mice (Fig. 3A and 3B). We also assessed PD-L1 expression by IHC staining in MDA-MB-231 xenograft tumor tissues from mice that had been treated with another PARPi, rucaparib, and harvested from our previous study (Du et al., 2016). Mice treated with rucaparib for 3 weeks had higher PD-L1 expression in their tumors compared with control mice (Fig. 3C). Together, these results indicated that PARPi upregulates PD-L1 expression in TNBC *in vitro* and *in vivo*.

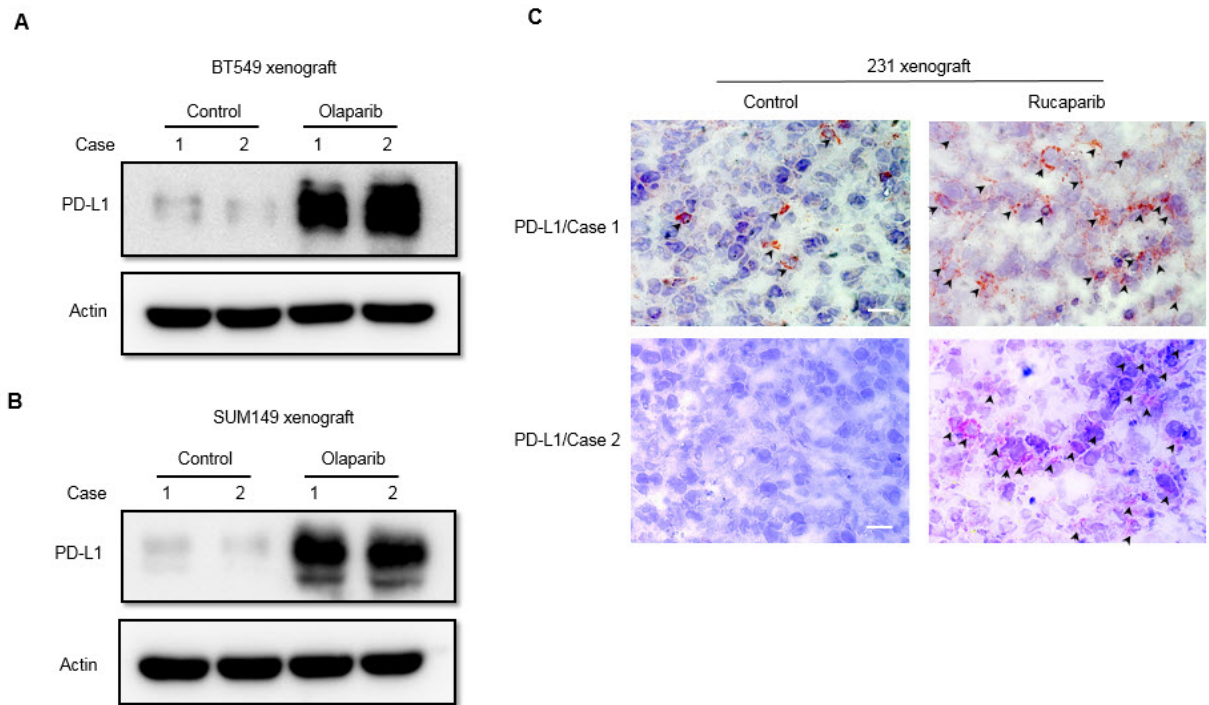


Figure 3. PARPi upregulates PD-L1 expression in xenograft tumors. (A) BT549, (B) SUM149 and (C) MDA-MB-231 cells were inoculated into mammary fad pad of nude mice, and the mice with established tumors were treated with olaparib or rucaparib. Tumors were then isolated to evaluate PD-L1 expression by immunoblotting (A and B) or IHC staining (C). Black arrowheads indicate the detected PD-L1 signals. Scale bar, 50 μ m.

3.2 PARPi-mediated PD-L1 upregulation primarily via GSK3 β inactivation

Next, we explored the mechanism underlying PARPi-enhanced PD-L1 protein expression. Multiple signaling pathways, such as STAT, NF- κ B and mTOR, have been reported to regulate PD-L1 expression level (Bellucci et al., 2013; Lim et al., 2016; Parsa et al., 2007). In an attempt to identify the potential signaling pathways that regulate PD-L1, we performed a phospho-kinase antibody array screen to identify kinases that are activated or inactivated following PARPi treatment. In the presence of PARPi treatment, the phosphorylation signal of GSK3 α/β at Ser21 and Ser9, which represents its inactivated form (Cohen and Frame, 2001), scored the second highest after the CHK2-p53 DNA repair pathway (Fig. 4A). CHK2 kinase is known to respond to DNA damage, and PARPi-induced CHK2 phosphorylation has previously been reported (Anderson et al., 2011; Hirao et al., 2000), further lending support to the results of our screen. The finding that PARPi inactivates GSK3 α/β is also in line with our recent report demonstrating inactivation of GSK3 β (p-Ser9) stabilizes PD-L1 (Li, 2016). Those findings together prompted us to investigate whether PARPi upregulates the expression of PD-L1 via inactivation of GSK3 β . To this end, we examined the status of GSK3 β phosphorylation at Ser9 in response to PARPi in SUM149 cells and BT549 cells by immunoblotting. The results indicated that PARPi treatment induced high GSK3 β Ser9 phosphorylation that was associated with PD-L1

upregulation (Fig. 4B and 4C). Knocking out GSK3 β significantly increased PD-L1 expression (Fig. 4C, lane 3 vs. 1). However, PD-L1 expression level in GSK3 β -knockout cells was no longer enhanced by olaparib treatment (Fig. 4C, lane 4 vs. 3). These results suggested that inactivation of GSK3 β is required for the PARPi-induced PD-L1 upregulation.

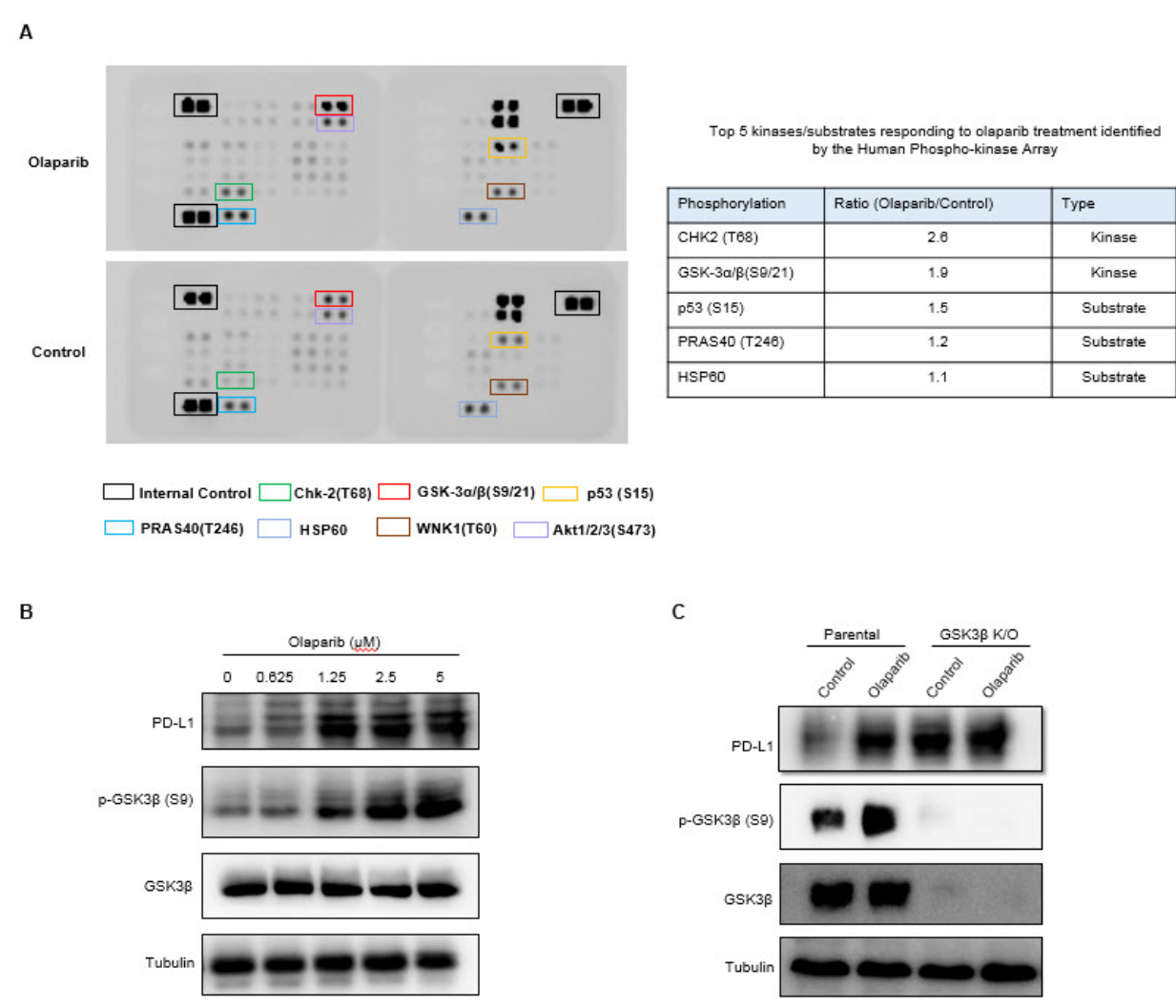


Figure 4. PARPi-mediated PD-L1 upregulation primarily via GSK3 β inactivation. (A)

SUM149 cells were treated with olaparib, and subjected to human phospho-Kinase Array.

The top two responding kinases were Chk2 and GSK3 α/β . (B) SUM149 cells were treated

with the indicated concentrations of olaparib for 10 days, and subjected to immunoblotting

with the indicated antibodies. (C) BT549 parental or GSK3 β knockout cells were treated

with 10 μ M olaparib for 24 hours. PD-L1 expression was evaluated by immunoblotting.

3.3 PARPi attenuates T-cell killing through PD-L1 induction

3.3.1 PARPi attenuates T-cell killing

To understand the functional significance of PD-L1 upregulation by PARPi, we first asked whether PARPi-induced PD-L1 increases PD-1 binding on cells. Exposure of MDA-MB-231 cells to olaparib induced more PD-1 binding to PD-L1 on the cell surface (Fig. 5A). Similar results were observed in MDA-MB-231 PARP1 K/D and K/O cells (Fig. 5B), and in SUM149 cells treated with different concentrations of olaparib (Fig. 5C). Next, to determine whether PARPi-mediated PD-L1 upregulation which resulted in increased PD-1 binding affects T-cell function, we performed a T-cell-mediated killing assay by co-culturing activated human peripheral blood mononuclear cells (PBMCs) with MDA-MB-231 cells labeled with nuclear red fluorescence protein (RFP; NucLight Red

MDA-MB-231) in the presence or absence of olaparib. As expected, olaparib efficiently inhibited cancer cell proliferation (black vs. blue in Fig. 5D, left panel; Fig. 6A) but did not inhibit activated PBMCs proliferation (Fig. 6B). Interestingly, although MDA-MB-231 cells were sensitive to the T-cell killing (black vs. red in Fig. 5D, left panel), those that were treated with olaparib were strongly resistant to activated T-cell killing (blue vs. yellow in Fig. 5D, left panel; Fig. 5D, right panel), supporting the notion that upregulation of PD-L1 by PARPi may render the PARPi-treated cancer cells more resistant to T-cell killing.

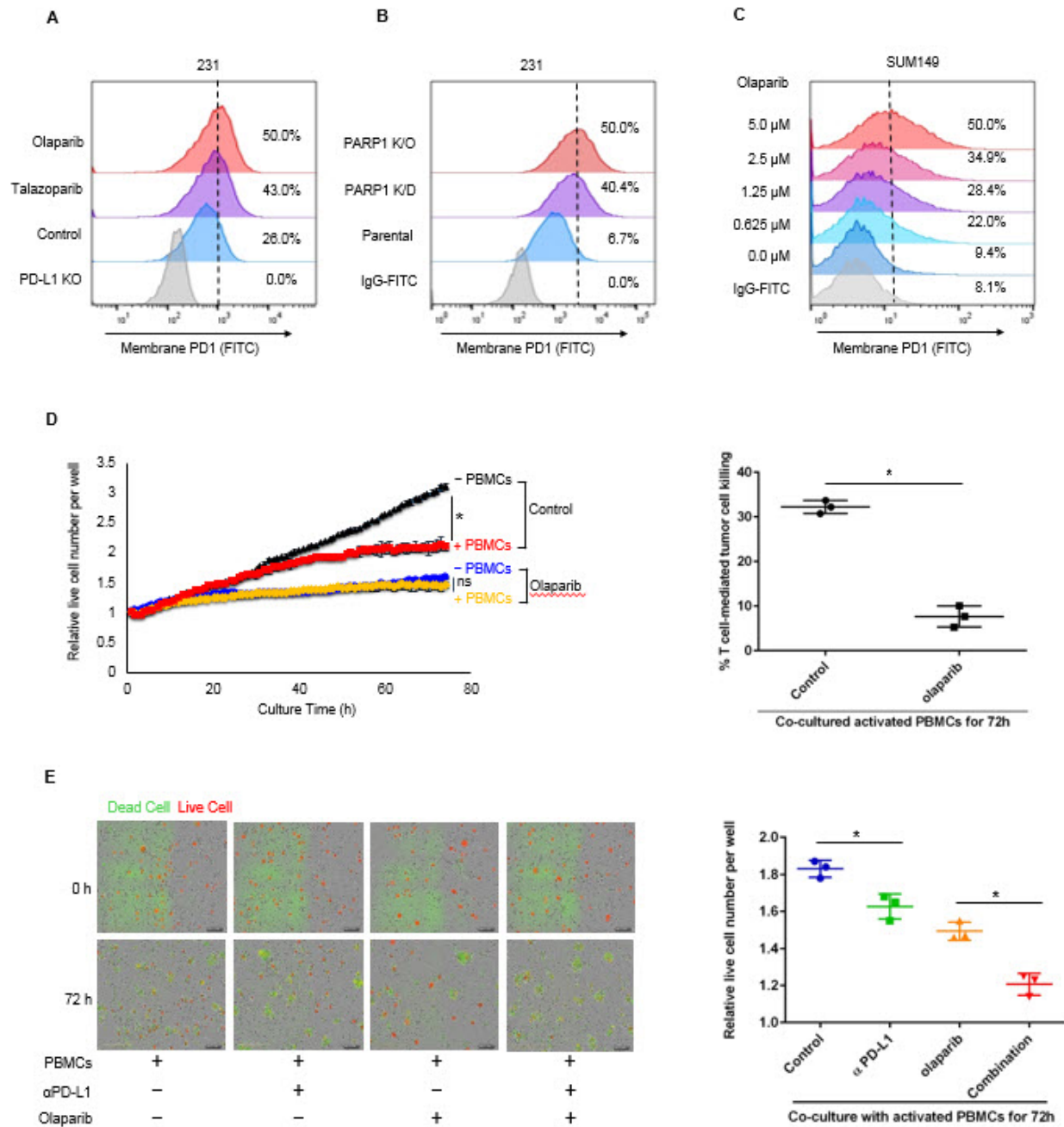


Figure 5. Olaparib increases PD-1 binding and attenuates T-cell-mediated cell death in TNBC cells. (A) FACS analysis of cell surface PD-1 binding of MDA-MB-231 cells treated with 10 μ M olaparib or 10 nM talazoparib for 24 hours. (B) FACS analysis of PARP1

knockdown (K/D), PARP1 knockout (K/O), and parental MDA-MB-231 cells. (C) SUM149 cells were treated with the indicated concentrations of olaparib for 10 days. (D) MDA-MB-231 cells expressing nuclear RFP protein were first treated with or without olaparib (10 μ M) for 3 hours and then co-cultured with or without activated peripheral blood mononuclear cells (PBMCs). Left, quantitation showing the number of live cells per well, counting the number of red fluorescent objects, normalized to that at the zero time point. Right, the percent of T cell-mediated tumor cell killing observed at 72 hours in activated PBMC co-culture with control or olaparib-treated cells (normalized to co-culture without PBMCs). (E) Left, representative merged images showing red fluorescent (nuclear restricted RFP), and green fluorescent (Caspase 3/7 substrate) objects in MDA-MB-231 cells co-cultured with activated PBMCs at 0 and 72 hours. Images were taken using the IncuCyte Zoom microscope. Right, quantitation showing the number of live cells following treatment with olaparib (10 μ M), PD-L1 antibody (PD-L1 Ab; 10 μ g/ml), or the combination co-cultured with activated PBMCs for 72 hours. The number of live cells (red fluorescent objects) were counted and normalized to that at the zero time point. * $P < 0.05$; ns, not significant.

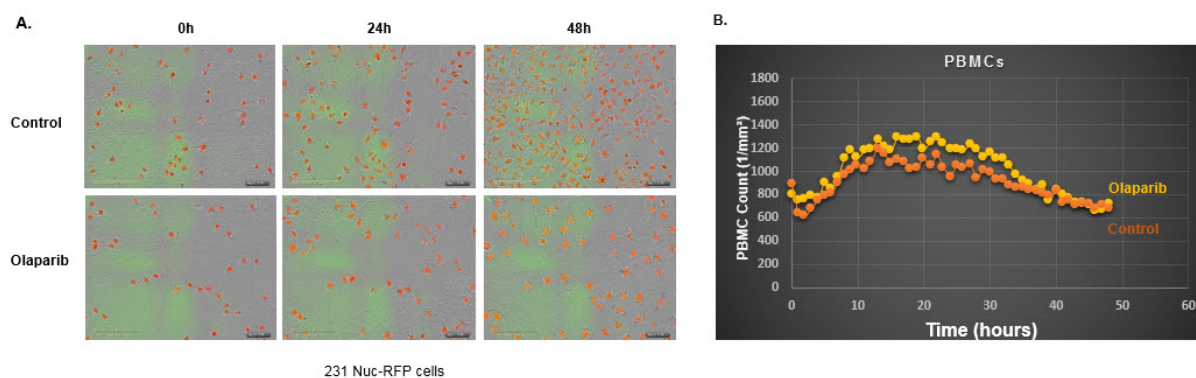


Figure 6. PARPi blocks cell proliferation of MDA-MB-231 cells but not activated PBMCs. (A) Representative images of MDA-MB-231 (Nuc-RFP) cells incubated with activated PBMCs treated with or without olaparib (10 μ M) at the indicated time points. Images were taken using the IncuCyte Zoom microscope. (B) Activated PBMCs were treated with or without olaparib (10 μ M). The IncuCyte Zoom microscope was used to take time-lapse images.

3.3.2 Blockade of PD-L1 re-sensitizes cancer cells treated with PARPi to T-cell killing

On the basis of the above results, we tested the T-cell killing effects of the combination of PD-L1 antibody and olaparib. The results showed that blockade of PD-L1 re-sensitized PARPi-treated MDA-MB-231 cells to activated T-cell killing, and that the PARPi-PD-L1 antibody combination was more effective than each agent alone (Fig. 5E).

3.4 Combination with PD-L1 blockade sensitizes PARPi therapy

Next, we sought to determine whether PD-L1 blockade could further potentiate PARPi anti-tumor efficacy *in vivo*. We first treated a murine breast cancer cell lines, EMT6, with olaparib with results showing significant induction of PD-L1 by olaparib (Fig. 7A). Consequently, we evaluated PARPi and anti-PD-L1 treatment alone or in combination in the EMT6 syngeneic mouse model. Consistent with our observations *in vitro*, both olaparib and anti-PD-L1 restricted tumor growth but the combined treatment demonstrated better therapeutic benefit than each treatment alone (Fig. 7B and 7C). There were significantly fewer Ki-67 positive tumor cells in the combined treatment compared with each treatment alone (Fig. 7D). Mice that received the combination treatment did not show any significant changes in body weight or elevation in liver enzyme (ALT and AST), and kidney toxicity marker, blood urea nitrogen (Fig. 8). At the end of treatment, tumors resected from mice were subjected to dissociation, and tumor cells and tumor-infiltrating lymphocytes (TIL) were separately harvested. Consistent with the observation in xenograft mice model (Fig. 2), PARPi significantly upregulated PD-L1 expression on tumor cell surface as determined by FACS in EMT6 syngeneic mice (Fig. 7E). Analysis of TILs by CyTOF showed that tumor-infiltrated cytotoxic CD8⁺ T-cell population, as measured by the level of IFN γ , decreased after PARPi treatment. Meanwhile, the addition of anti-PD-L1 restored the

cytotoxic CD8⁺ T-cell population (Fig. 8F). These results suggested that PARPi enhances cancer-associated immunosuppression through upregulation of PD-L1 and that PD-L1 blockade potentiates PARPi therapy.

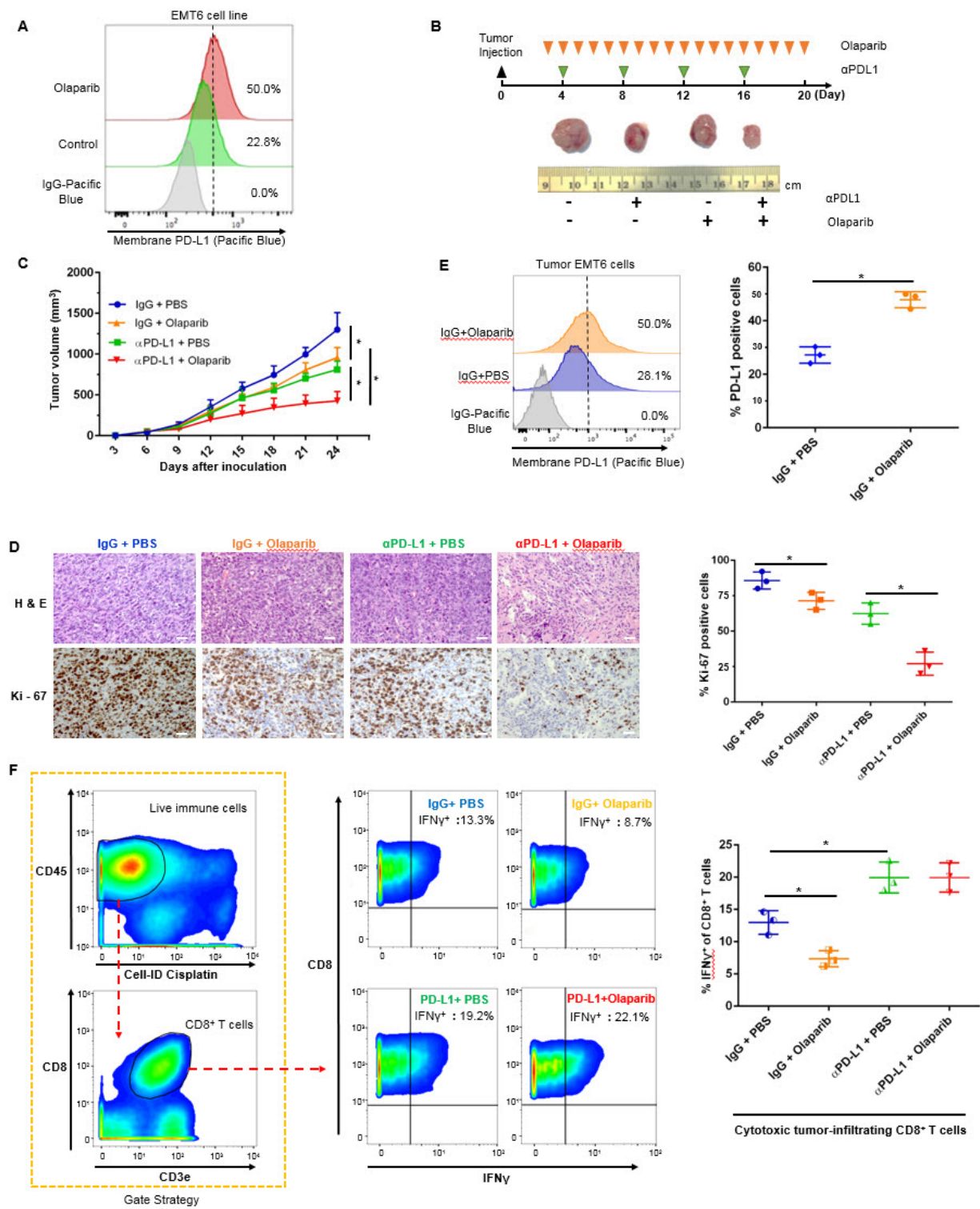


Figure 7. PARPi-induced PD-L1 upregulation suppresses anticancer immunity and blockade of PD-L1 potentiates PARPi. (A) EMT6 cells were treated with 10 μ M olaparib

for 24 h. Cell surface PD-L1 were analyzed by FACS. (B) Representative images of tumors after olaparib and/or anti-PD-L1 antibody treatment at the indicated time points in the EMT6 syngeneic mouse model. (C) Effects of olaparib and/or anti-PD-L1 antibody treatment on tumor growth in EMT6 syngeneic mouse model treated (n = 8). Tumors were measured at the indicated time points and dissected for tumor cell PD-L1 expression analysis, TIL analysis, and pathological analysis at endpoint. (D) Hematoxylin and eosin (H&E) and Ki-67 staining of EMT6 tumors. Scale bar, 50 μ m. (E) Cell surface PD-L1 expression in EMT6 cells derived from EMT6 mouse tumors. (F) Cytotoxic CD8⁺ T cells population (IFN γ ⁺ CD8⁺ CD3⁺ CD45⁺) in TILs isolated from EMT6 tumors by CyTOF analysis. * P < 0.05

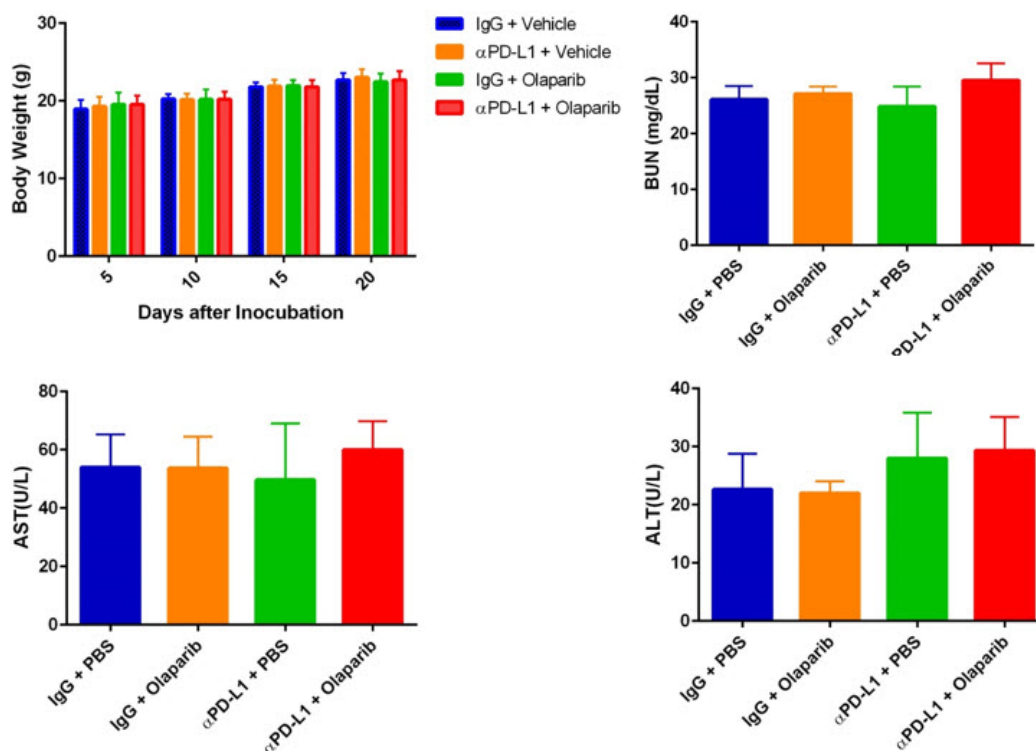
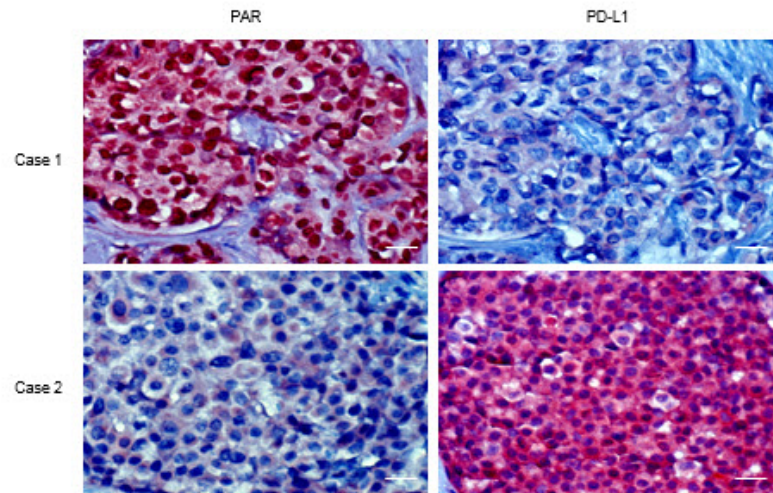


Figure 8. Toxicity assessment of treatment on BALB/c mice. The body weight was measured every 5 days, and mice liver, and kidney functions were tested at the end of the experiments. BUN, blood urea nitrogen; ALT, alanine aminotransferase; AST, aspartate aminotransferase.

3.5 Correlations of PARylation and PD-L1 expression in human tumor tissues

PARP exerts its biological function through its PARylation enzyme activity, and PARP inhibitors are designed to inhibit its enzyme activity. Thus, the extent of protein PARylation was utilized to assess the efficacy of PARP inhibition (Kummar et al., 2011). To further validate our findings in human cancer patient samples, we analyzed the correlations between PARylation level and PD-L1 expression in human breast tumor specimens using IHC. High level of protein PARylation was detected in 87 (75.0%) of the 116 specimens, of which 65 (74.7%) cases showed low PD-L1 expression (Figure 9, top). The Pearson Chi-Square test further showed the inverse correlation between PARylation level and PD-L1 expression exists in human cancer patient specimens (Figure 9, bottom). These results supported the notion that high PARP enzyme activity suppresses PD-L1 expression.



		PAR		Total	P value
		- / +	++ / +++		
PD-L1	- / +	15 (12.9%)	65 (56.0%)	80 (69.0%)	P = 0.02
	++ / +++	14 (12.1%)	22 (19.0%)	36 (31.0%)	
	Total	29 (25.0%)	87 (75.0%)	116 (100%)	

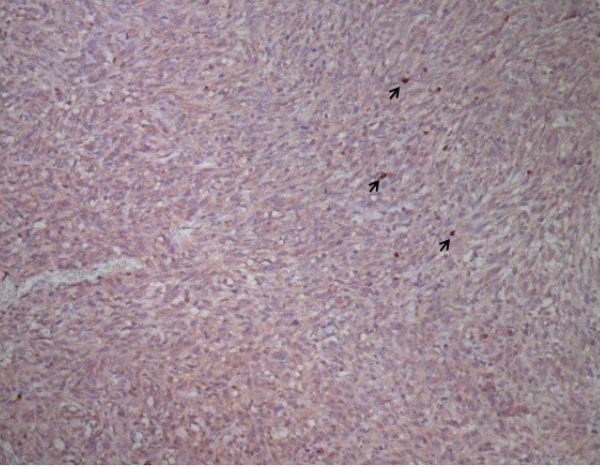
Figure 9. Inverse correlation between PAR and PD-L1 in surgical specimens of breast cancer. Top, representative images of IHC staining of PAR and PD-L1 in human breast cancer tissues (n = 116). Scale bar, 50 μ m. Bottom, correlation analysis between PAR and PDL-1 was analyzed using the Pearson Chi-Square test (P = 0.02). A P value of less than 0.05 was considered to be statistically significant.

3.6 PARPi treatment increases T lymphocytes infiltration in tumors

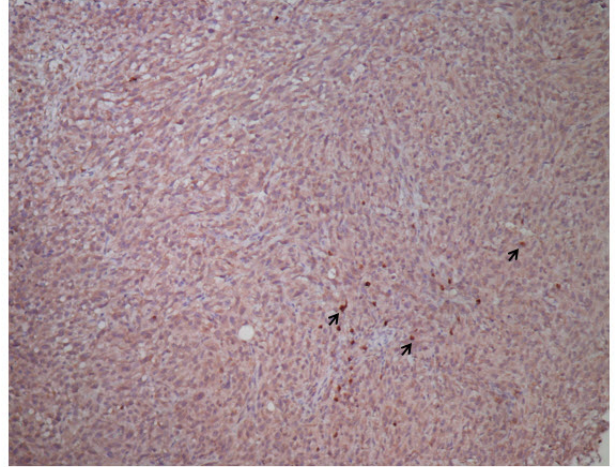
IHC staining of CD3 demonstrates that EMT6 tumors under PARPi treatment showed increased T cell infiltration compared with those under control treatment (Fig. 10). The potential reasons may be: PARPi promotes cancer cell death via its cytotoxic effects to release more antigens and attract lymphocytes infiltration; as a DNA repair enzyme inhibitor, PARPi may lead to more DNA damage, increase the mutation burden and promote neo-antigen generation.

As shown in Fig. 7F, PARPi treatment decrease the percentage of cytotoxic CD8 T cells population (indicated as IFN γ ⁺ CD8⁺ T population) against total CD8 T cells, partly due to the PARPi-mediated upregulation of PD-L1 on cancer cells. Taken together, these data indicate that on one hand PARPi increases T lymphocyte infiltration in tumors; however on the other hand PARPi upregulates PD-L1 expression on tumor cells which limits the anti-tumor effects of the infiltrating T lymphocytes, indicated by lower cytotoxic CD8 T cell percentage. Therefore, the addition of PD-L1 or PD-1 blockade to PARPi therapy can greatly improve the anti-tumor effects via attenuating the cancer-associated immunosuppression.

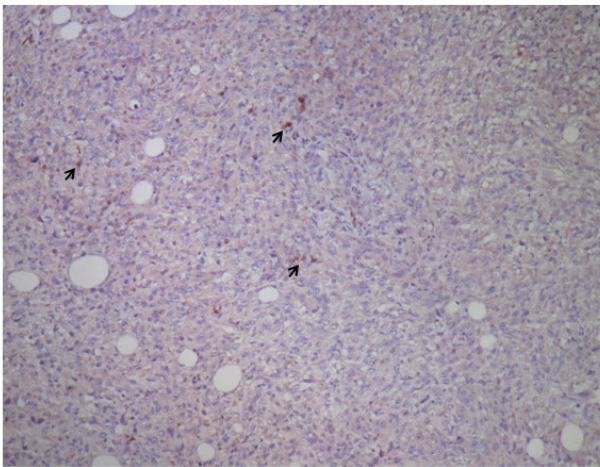
A



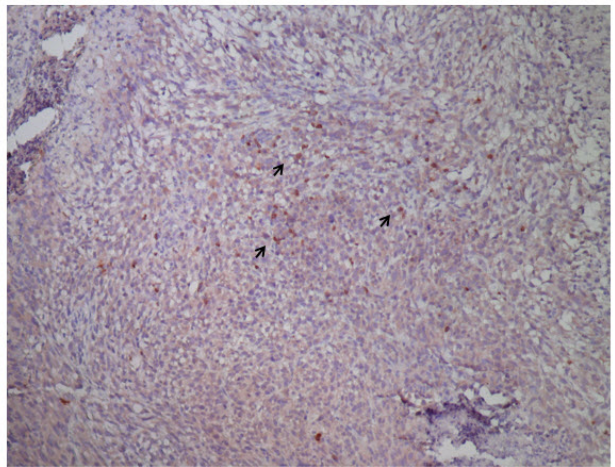
B



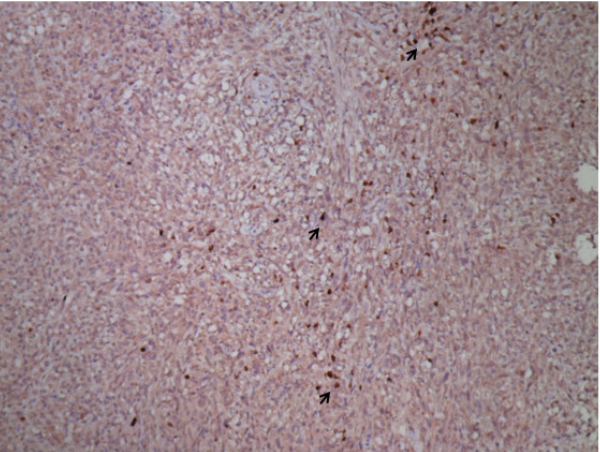
C



D



E



F

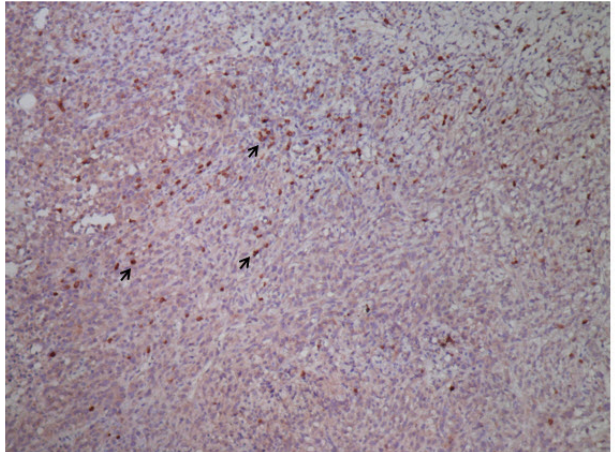


Figure 10. PARPi treatment increases T lymphocytes infiltration in EMT6 tumors. IHC

staining of CD3 in mouse tumor tissues from three EMT6 syngeneic BABL/c mice (A, B and C) under control treatment, or (D, E and F) under PARPi treatment. Three representative black arrows in each panel indicate detected CD3 signals.

3.7 PARPi upregulates PD-L1 in specific cancer cell lines

Fig. 2 and 3 showed that PARPi can upregulate in three breast cancer cell lines, MDA-MB-231, BT549 and SUM149. However, cell surface level of PD-L1 was not upregulated in one breast cancer cell line T47D after PARPi treatment (Fig. 11B). Since PARPi is clinically used in ovarian cancer and also shows promising clinical benefit in prostate cancer demonstrated by late-stage clinical trials, ovarian cancer cell lines HOC7 and OVCA433, and prostate cancer cell lines PC3 and DU145 were further tested. PARPi mediated PD-L1 upregulation can be observed in HOC7 and PC3 cells but not OVCA433 or DU145 cells (Fig. 11A). H460, HELA and U2OS were also treated with 10 μ M olaparib for 72 h. It showed that olaparib can upregulate PD-L1 in HELA and U2OS cells. In addition, in murine breast cancer cell lines, there is a more obvious induction of PD-L1 by olaparib in EMT6 cells compared with 4T1 cells (Fig. 12). In sum, PARPi upregulates PD-L1 in specific cancer cell lines.

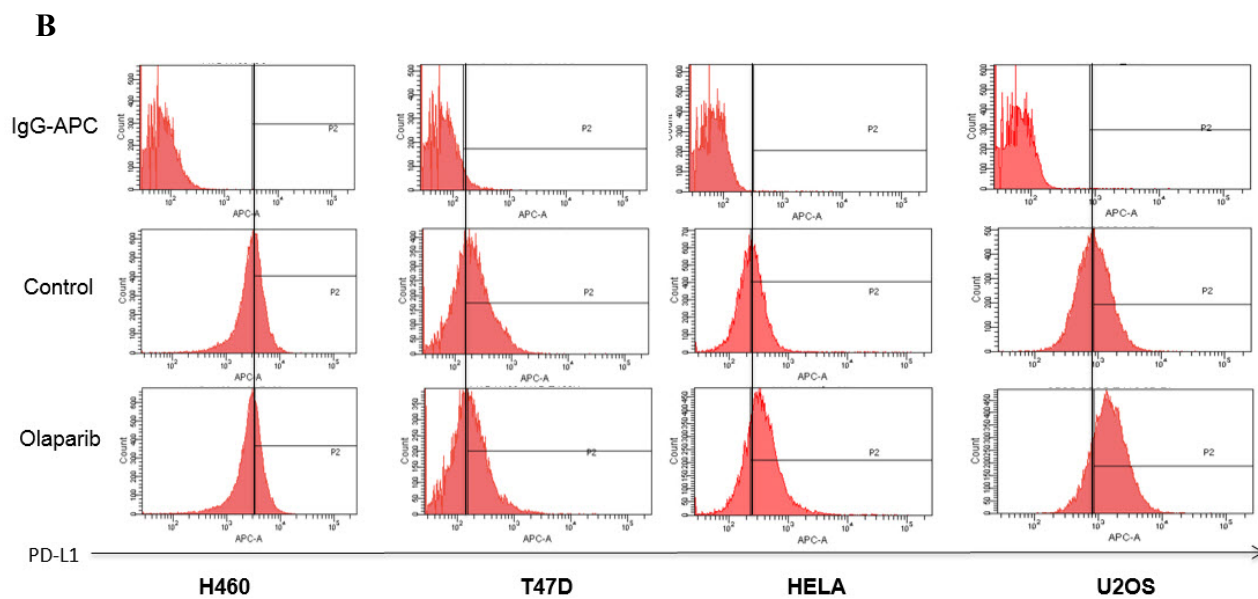
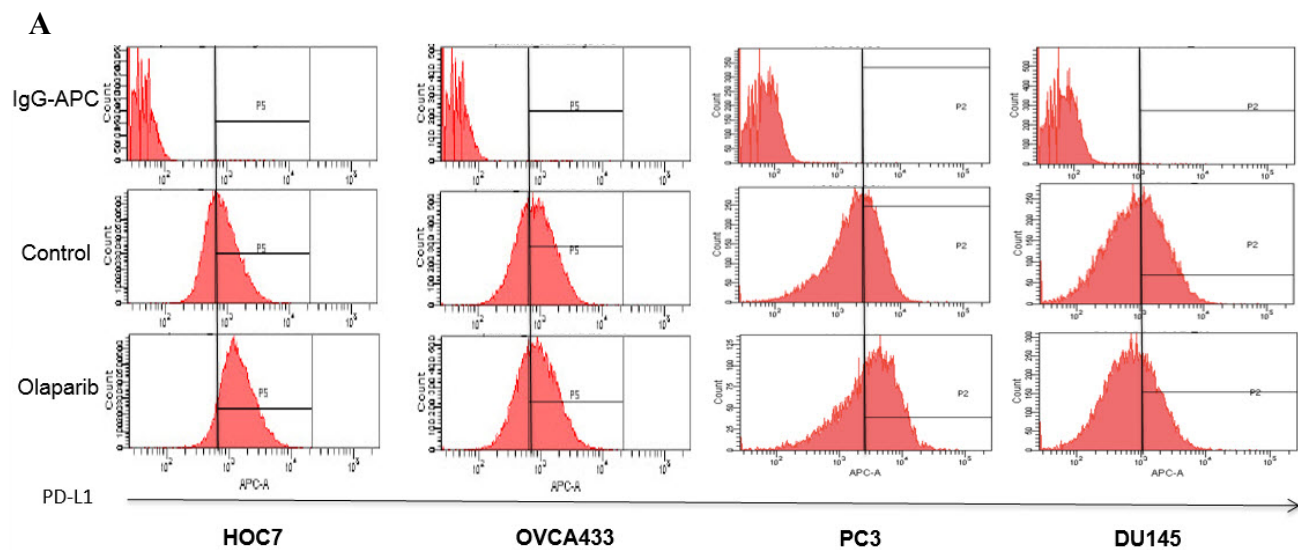


Figure 11. PARPi upregulates PD-L1 expression in specific cancer cell lines. (A) Ovarian cancer cell lines HOC7 and OVCA433, and prostate cancer cell lines PC3 and DU145 were treated with 10 μ M olaparib for 72 h. Cell surface PD-L1 were measured by FACS analysis. Olaparib can induce PD-L1 upregulation in HOC7 and PC3 cancer cells but not OVCA433 or DU145 cells. (B) H460, T47D, HELA and U2OS were treated with 10 μ M olaparib for 72 h. Olaparib can upregulate PD-L1 in HELA and U2OS cells.

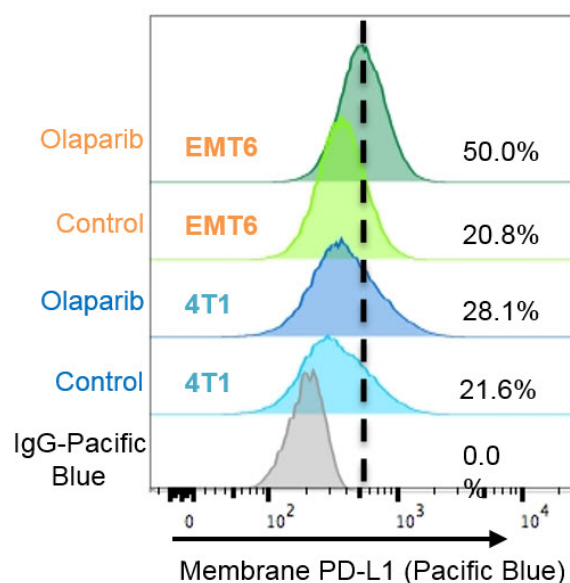


Figure 12. A more obvious induction of PD-L1 was observed in EMT6 cancer cells compared with 4T1 cells. Murine breast cancer cells were treated with 10 μ M olaparib for 72 h

Chapter 4

Conclusion and Discussion

Although the cytotoxic effects of PARPi have been well studied, the role of PARP inhibition in cancer-associated immunity is still largely unknown. In this study, we demonstrated that PARPi upregulates PD-L1 expression primarily through GSK3 β inactivation. PARPi renders cancer cells more resistant to T-cell-mediated cell death, and PD-L1 blockade potentiates PARPi *in vitro* and *in vivo*. These data strongly suggested that PD-L1 upregulation by PARPi treatment attenuates PARPi therapeutic efficacy via tumor-associated immunosuppression, and simultaneous inhibition of PARP and PD-L1 may benefit breast cancer patients. There are currently three clinical trials testing the combination of PARPi (olaparib, niraparib, and BGB-290) and PD-L1 or PD-1 antibody in multiple cancer types (NCT02484404; NCT02657889; NCT02660034). The results of the current study provided scientific basis for these clinical trials.

Higuchi et al. recently investigated the combination of PARPi and CTLA4 antibody in the BR5-AKT ovarian cancer syngeneic mouse model and claimed to have observed a synergistic therapeutic effect (Higuchi et al., 2015); however, they indicated they did not observe such synergistic effect using the anti-PD-1 and PARPi combination in the same animal model. It is worthwhile to mention that PD-1 blockade in the BR5-AKT syngeneic mice did not affect T-cell activation or cytokine induction in the peritoneal tumor environment in their study [28], and therefore, synergistic effects may not be observed in

combination with PARPi under their experimental condition. In contrast, the results from our study indicated that PARPi upregulates PD-L1 in EMT6 tumors and PD-L1 blockade attenuated immunosuppression activity (Fig. 5F), which allowed us to observe an anti-PD-L1 therapy-potentiated antitumor activity of PARPi. Meanwhile, other studies have reported that chemotherapeutic agents, gemcitabine and paclitaxel, can induce PD-L1 in ovarian cancer cells (Ding et al., 2014; Peng et al., 2015). The combination of paclitaxel and PD-L1/PD-1 blockade enhanced antitumor efficacy in an ID8 ovarian syngeneic mouse model (Peng et al., 2015). Therefore, whether the combination of PD-L1 blockade and PARPi induces synergistic effect in ovarian cancer warrants further investigation in a suitable animal model. Nonetheless, the mechanism of interaction between PARP and PD-L1/PD-1 as shown in the current study is timely and provides scientific basis to develop more effective combination therapies consisting of two powerful anti-cancer agents.

In this study, it has been shown that PARPi treatment increases T lymphocytes infiltration in syngeneic mouse tumors. However, the PARPi-induced PD-L1 on tumor cells serves as “side effects”, inhibits the T cell activation and attenuates the anti-tumor effects of the infiltrating T lymphocytes. Therefore, the addition of anti-PD-L1 or anti-PD-1 therapy to PARPi can greatly enhance therapeutic efficacy via blocking the cancer-associated

immunosuppression. However, the underlying mechanisms of how PARPi increases T cell infiltration needs further study.

It has also been observed that PARPi-mediated PD-L1 induction is applied to specific cancer cell lines. It is quite possible that human tumors that treated with PARPi can be classified as tumors with PD-L1 induction or those without induction. Future studies should focus on the unique features of the tumors with or without PARPi-mediated PD-L1 induction, and consequently identify biomarkers to distinguish the two types of tumors. Tumors with PD-L1 induction after PARPi treatment should benefit more from the combination of PD-L1 or PD-1 blockade and PARPi. Therefore, the identified biomarkers can be used to stratify patients for the anti-PD-L1/ PD-1 and PARPi combination therapy.

Chapter 5 Bibliography

Anderson, V.E., M.I. Walton, P.D. Eve, K.J. Boxall, L. Antoni, J.J. Caldwell, W. Aherne, L.H.

Pearl, A.W. Oliver, I. Collins, and M.D. Garrett. 2011. CCT241533 is a potent and selective inhibitor of CHK2 that potentiates the cytotoxicity of PARP inhibitors. *Cancer Res.* 71:463-472.

Bellucci, R., A. Martin, D. Bommarito, K.S. Wang, G.J. Freeman, and J. Ritz. 2013. JAK1 and JAK2 Modulate Tumor Cell Susceptibility To Natural Killer (NK) Cells Through Regulation Of PDL1 Expression. *Blood.* 122.

Bryant, H.E., E. Petermann, N. Schultz, A.S. Jemth, O. Loseva, N. Issaeva, F. Johansson, S. Fernandez, P. McGlynn, and T. Helleday. 2009. PARP is activated at stalled forks to mediate Mre11-dependent replication restart and recombination. *EMBO J.* 28:2601-2615.

Cohen, P., and S. Frame. 2001. The renaissance of GSK3. *Nat Rev Mol Cell Biol.* 2:769-776.

Ding, Z.C., X.Y. Lu, M. Yu, H. Lemos, L. Huang, P. Chandler, K.B. Liu, M. Walters, A. Krasinski, M. Mack, B.R. Blazar, A.L. Mellor, D.H. Munn, and G. Zhou. 2014. Immunosuppressive Myeloid Cells Induced by Chemotherapy Attenuate Antitumor CD4(+) T-Cell Responses through the PD-1-PD-L1 Axis. *Cancer Research.* 74:3441-3453.

Dong, H., S.E. Strome, D.R. Salomao, H. Tamura, F. Hirano, D.B. Flies, P.C. Roche, J. Lu, G. Zhu, K. Tamada, V.A. Lennon, E. Celis, and L. Chen. 2002. Tumor-associated B7-H1 promotes T-cell apoptosis: a potential mechanism of immune evasion. *Nat Med*. 8:793-800.

Du, Y., H. Yamaguchi, Y. Wei, J.L. Hsu, H.L. Wang, Y.H. Hsu, W.C. Lin, W.H. Yu, P.G. Leonard, G.R.t. Lee, M.K. Chen, K. Nakai, M.C. Hsu, C.T. Chen, Y. Sun, Y. Wu, W.C. Chang, W.C. Huang, C.L. Liu, Y.C. Chang, C.H. Chen, M. Park, P. Jones, G.N. Hortobagyi, and M.C. Hung. 2016. Blocking c-Met-mediated PARP1 phosphorylation enhances anti-tumor effects of PARP inhibitors. *Nat Med*. 22:194-201.

Edwards, S.L., R. Brough, C.J. Lord, R. Natrajan, R. Vatcheva, D.A. Levine, J. Boyd, J.S. Reis, and A. Ashworth. 2008. Resistance to therapy caused by intragenic deletion in BRCA2. *Nature*. 451:1111-U1118.

Freeman, G.J., A.J. Long, Y. Iwai, K. Bourque, T. Chernova, H. Nishimura, L.J. Fitz, N. Malenkovich, T. Okazaki, M.C. Byrne, H.F. Horton, L. Fouser, L. Carter, V. Ling, M.R. Bowman, B.M. Carreno, M. Collins, C.R. Wood, and T. Honjo. 2000. Engagement of the PD-1 immunoinhibitory receptor by a novel B7 family member

leads to negative regulation of lymphocyte activation. *The Journal of experimental medicine*. 192:1027-1034.

Galluzzi, L., A. Buque, O. Kepp, L. Zitvogel, and G. Kroemer. 2015. Immunological Effects of Conventional Chemotherapy and Targeted Anticancer Agents. *Cancer Cell*. 28:690-714.

Garon, E.B., N.A. Rizvi, R.N. Hui, N. Leighl, A.S. Balmanoukian, J.P. Eder, A. Patnaik, C. Aggarwal, M. Gubens, L. Horn, E. Carcereny, M.J. Ahn, E. Felip, J.S. Lee, M.D. Hellmann, O. Hamid, J.W. Goldman, J.C. Soria, M. Dolled-Filhart, R.Z. Rutledge, J. Zhang, J.K. Luceford, R. Rangwala, G.M. Lubiniecki, C. Roach, K. Emancipator, L. Gandhi, and K.-. Investigators. 2015. Pembrolizumab for the Treatment of Non-Small-Cell Lung Cancer. *New Engl J Med*. 372:2018-2028.

Higuchi, T., D.B. Flies, N.A. Marjon, G. Mantia-Smaldone, L. Ronner, P.A. Gimotty, and S.F. Adams. 2015. CTLA-4 Blockade Synergizes Therapeutically with PARP Inhibition in BRCA1-Deficient Ovarian Cancer. *Cancer immunology research*. 3:1257-1268.

Hirao, A., Y.Y. Kong, S. Matsuoka, A. Wakeham, J. Ruland, H. Yoshida, D. Liu, S.J. Elledge, and T.W. Mak. 2000. DNA damage-induced activation of p53 by the checkpoint kinase Chk2. *Science*. 287:1824-1827.

Hodi, F.S. 2010. Improved Survival with Ipilimumab in Patients with Metastatic Melanoma (vol 363, pg 711, 2010). *New Engl J Med*. 363:1290-1290.

Ibrahim, Y.H., C. Garcia-Garcia, V. Serra, L. He, K. Torres-Lockhart, A. Prat, P. Anton, P. Cozar, M. Guzman, J. Grueso, O. Rodriguez, M.T. Calvo, C. Aura, O. Diez, I.T. Rubio, J. Perez, J. Rodon, J. Cortes, L.W. Ellisen, M. Scaltriti, and J. Baselga. 2012. PI3K Inhibition Impairs BRCA1/2 Expression and Sensitizes BRCA-Proficient Triple-Negative Breast Cancer to PARP Inhibition. *Cancer Discovery*. 2:1036-1047.

Jaspers, J.E., A. Kersbergen, U. Boon, W. Sol, L. van Deemter, S.A. Zander, R. Drost, E. Wientjens, J. Ji, A. Aly, J.H. Doroshov, A. Cranston, N.M. Martin, A. Lau, M.J. O'Connor, S. Ganesan, P. Borst, J. Jonkers, and S. Rottenberg. 2013. Loss of 53BP1 causes PARP inhibitor resistance in Brca1-mutated mouse mammary tumors. *Cancer Discov*. 3:68-81.

Jiao, S., W. Xia, H. Yamaguchi, Y. Wei, M.K. Chen, J.M. Hsu, J.L. Hsu, W.H. Yu, Y. Du, H.H. Lee, C.W. Li, C.K. Chou, S.O. Lim, S.S. Chang, J.K. Litton, B. Arun, G.N. Hortobagyi, and M.C. Hung. 2017. PARP inhibitor upregulates PD-L1 expression and enhances cancer-associated immunosuppression. *Clin Cancer Res*.

Juvekar, A., L.N. Burga, H. Hu, E.P. Lunsford, Y.H. Ibrahim, J. Balmana, A. Rajendran, A. Papa, K. Spencer, C.A. Lyssiotis, C. Nardella, P.P. Pandolfi, J. Baselga, R. Scully,

- J.M. Asara, L.C. Cantley, and G.M. Wulf. 2012. Combining a PI3K Inhibitor with a PARP Inhibitor Provides an Effective Therapy for BRCA1-Related Breast Cancer. *Cancer Discovery*. 2:1048-1063.
- Karnak, D., C.G. Engelke, L.A. Parsels, T. Kausar, D. Wei, J.R. Robertson, K.B. Marsh, M.A. Davis, L. Zhao, J. Maybaum, T.S. Lawrence, and M.A. Morgan. 2014. Combined inhibition of Wee1 and PARP1/2 for radiosensitization in pancreatic cancer. *Clin Cancer Res*. 20:5085-5096.
- Kaufman, B., R. Shapira-Frommer, R.K. Schmutzler, M.W. Audeh, M. Friedlander, J. Balmana, G. Mitchell, G. Fried, S.M. Stemmer, A. Hubert, O. Rosengarten, M. Steiner, N. Loman, K. Bowen, A. Fielding, and S.M. Domchek. 2015. Olaparib monotherapy in patients with advanced cancer and a germline BRCA1/2 mutation. *J Clin Oncol*. 33:244-250.
- Kim, G., G. Ison, A.E. McKee, H. Zhang, S. Tang, T. Gwise, R. Sridhara, E. Lee, A. Tzou, R. Philip, H.J. Chiu, T.K. Ricks, T. Palmby, A.M. Russell, G. Ladouceur, E. Pfuma, H. Li, L. Zhao, Q. Liu, R. Venugopal, A. Ibrahim, and R. Pazdur. 2015. FDA Approval Summary: Olaparib Monotherapy in Patients with Deleterious Germline BRCA-Mutated Advanced Ovarian Cancer Treated with Three or More Lines of Chemotherapy. *Clin Cancer Res*. 21:4257-4261.

Kummar, S., A. Chen, J.P. Ji, Y.P. Zhang, J.M. Reid, M. Ames, L. Jia, M. Weil, G. Speranza, A.J. Murgo, R. Kinders, L.H. Wang, R.E. Parchment, J. Carter, H. Stotler, L. Rubinstein, M. Hollingshead, G. Melillo, Y. Pommier, W. Bonner, J.E. Tomaszewski, and J.H. Doroshow. 2011. Phase I Study of PARP Inhibitor ABT-888 in Combination with Topotecan in Adults with Refractory Solid Tumors and Lymphomas. *Cancer Research*. 71:5626-5634.

Li, C.W., Lim SO, Xia W, Lee HH, Li CC, Kuo CW, et al. 2016. Glycosylation and stabilization of programmed death ligand-1 suppresses T-cell activity. *Nat Commun*. 7:12632.

Lim, S.O., C.W. Li, W. Xia, J.H. Cha, L.C. Chan, Y. Wu, S.S. Chang, W.C. Lin, J.M. Hsu, Y.H. Hsu, T. Kim, W.C. Chang, J.L. Hsu, H. Yamaguchi, Q. Ding, Y. Wang, Y. Yang, C.H. Chen, A.A. Sahin, D. Yu, G.N. Hortobagyi, and M.C. Hung. 2016. Deubiquitination and Stabilization of PD-L1 by CSN5. *Cancer Cell*.

Mirza, M.R., B.J. Monk, J. Herrstedt, A.M. Oza, S. Mahner, A. Redondo, M. Fabbro, J.A. Ledermann, D. Lorusso, I. Vergote, N.E. Ben-Baruch, C. Marth, R. Madry, R.D. Christensen, J.S. Berek, A. Dorum, A.V. Tinker, A. du Bois, A. Gonzalez-Martin, P. Follana, B. Benigno, P. Rosenberg, L. Gilbert, B.J. Rimel, J. Buscema, J.P. Balser, S.

- Agarwal, U.A. Matulonis, and E.-O.N. Investigators. 2016. Niraparib Maintenance Therapy in Platinum-Sensitive, Recurrent Ovarian Cancer. *N Engl J Med*.
- Muvarak, N.E., K. Chowdhury, L. Xia, C. Robert, E.Y. Choi, Y. Cai, M. Bellani, Y. Zou, Z.N. Singh, V.H. Duong, T. Rutherford, P. Nagaria, S.M. Bentzen, M.M. Seidman, M.R. Baer, R.G. Lapidus, S.B. Baylin, and F.V. Rassool. 2016. Enhancing the Cytotoxic Effects of PARP Inhibitors with DNA Demethylating Agents - A Potential Therapy for Cancer. *Cancer Cell*. 30:637-650.
- Paddock, M.N., A.T. Bauman, R. Higdon, E. Kolker, S. Takeda, and A.M. Scharenberg. 2011. Competition between PARP-1 and Ku70 control the decision between high-fidelity and mutagenic DNA repair. *DNA Repair (Amst)*. 10:338-343.
- Parsa, A.T., J.S. Waldron, A. Panner, C.A. Crane, I.F. Parney, J.J. Barry, K.E. Cachola, J.C. Murray, T. Tihan, M.C. Jensen, P.S. Mischel, D. Stokoe, and R.O. Pieper. 2007. Loss of tumor suppressor PTEN function increases B7-H1 expression and immunoresistance in glioma. *Nat Med*. 13:84-88.
- Peng, J., J. Hamanishi, N. Matsumura, K. Abiko, K. Murat, T. Baba, K. Yamaguchi, N. Horikawa, Y. Hosoe, S.K. Murphy, I. Konishi, and M. Mandai. 2015. Chemotherapy Induces Programmed Cell Death-Ligand 1 Overexpression via the Nuclear

Factor-kappaB to Foster an Immunosuppressive Tumor Microenvironment in Ovarian Cancer. *Cancer Res.* 75:5034-5045.

Reck, M., D. Rodriguez-Abreu, A.G. Robinson, R. Hui, T. Csoszi, A. Fulop, M. Gottfried, N. Peled, A. Tafreshi, S. Cuffe, M. O'Brien, S. Rao, K. Hotta, M.A. Leiby, G.M. Lubiniecki, Y. Shentu, R. Rangwala, J.R. Brahmer, and K.-. Investigators. 2016. Pembrolizumab versus Chemotherapy for PD-L1-Positive Non-Small-Cell Lung Cancer. *N Engl J Med.*

Robert, C., G.V. Long, B. Brady, C. Dutriaux, M. Maio, L. Mortier, J.C. Hassel, P. Rutkowski, C. McNeil, E. Kalinka-Warzocha, K.J. Savage, M.M. Hernberg, C. Lebbe, J. Charles, C. Mihalcioiu, V. Chiarion-Sileni, C. Mauch, F. Cognetti, A. Arance, H. Schmidt, D. Schadendorf, H. Gogas, L. Lundgren-Eriksson, C. Horak, B. Sharkey, I.M. Waxman, V. Atkinson, and P.A. Ascierto. 2015. Nivolumab in Previously Untreated Melanoma without BRAF Mutation. *New Engl J Med.* 372:320-330.

Rosenberg, J.E., J. Hoffman-Censits, T. Powles, M.S. van der Heijden, A.V. Balar, A. Necchi, N. Dawson, P.H. O'Donnell, A. Balmanoukian, Y. Loriot, S. Srinivas, M.M. Retz, P. Grivas, R.W. Joseph, M.D. Galsky, M.T. Fleming, D.P. Petrylak, J.L. Perez-Gracia, H.A. Burris, D. Castellano, C. Canil, J. Bellmunt, D. Bajorin, D. Nickles, R. Bourgon,

- G.M. Frampton, N. Cui, S. Mariathasan, O. Abidoye, G.D. Fine, and R. Dreicer. 2016. Atezolizumab in patients with locally advanced and metastatic urothelial carcinoma who have progressed following treatment with platinum-based chemotherapy: a single-arm, multicentre, phase 2 trial. *Lancet*. 387:1909-1920.
- Sonnenblick, A., E. de Azambuja, H.A. Azim, Jr., and M. Piccart. 2015. An update on PARP inhibitors--moving to the adjuvant setting. *Nat Rev Clin Oncol*. 12:27-41.
- Topalian, S.L., C.G. Drake, and D.M. Pardoll. 2012. Targeting the PD-1/B7-H1(PD-L1) pathway to activate anti-tumor immunity. *Curr Opin Immunol*. 24:207-212.
- Tutt, A., M. Robson, J.E. Garber, S.M. Domchek, M.W. Audeh, J.N. Weitzel, M. Friedlander, B. Arun, N. Loman, R.K. Schmutzler, A. Wardley, G. Mitchell, H. Earl, M. Wickens, and J. Carmichael. 2010. Oral poly(ADP-ribose) polymerase inhibitor olaparib in patients with BRCA1 or BRCA2 mutations and advanced breast cancer: a proof-of-concept trial. *Lancet*. 376:235-244.
- Xia, W., J.S. Chen, X. Zhou, P.R. Sun, D.F. Lee, Y. Liao, B.P. Zhou, and M.C. Hung. 2004. Phosphorylation/cytoplasmic localization of p21Cip1/WAF1 is associated with HER2/neu overexpression and provides a novel combination predictor for poor prognosis in breast cancer patients. *Clin Cancer Res*. 10:3815-3824.

Chapter 6 Vita

Shiping Jiao was born in Liaoning Province, China, on December 1990. He received his Bachelor of Medicine degree (Equivalent to M.D. in U.S.A) from Zhongshan School of medicine, Sun Yat-sen University in June 2015. During his study in medical school, he did summer research about cancer targeted gene therapy in Sun Yat-sen University Cancer Center. He enrolled The University of Texas MD Anderson Cancer Center UTHealth Graduate School of Biomedical Sciences in September 2015. During his study in MD Anderson Cancer Center, he focused on the immune checkpoint therapy and the resistance to targeted inhibitors in cancer.

Permanent address:

602, ChengTai WenJiao No. 13 - 4,
Dong ChangChun Road.
WaFang Dian, Dalian 116200
China